Journal of Advanced Ceramics
2022, **11**(9): 1491–1497
https://doi.org/10.1007/s40145-022-0616-0
ISSN 2226-4108
CN 10-1154/TQ

Rapid Communication

Facile synthesis of hollow Ti_3AlC_2 microrods in molten salts via Kirkendall effect

Yi LIU[a,*], Chuangye WANG[a], Wei LUO[a], Liang BAI[a], Yang XU[b], Xiaodong HAO[b], Jianfeng ZHU[a], Shouwu GUO[a,c]

[a]*School of Materials Science and Engineering, Shaanxi University of Science and Technology, Xi'an 710021, China*
[b]*Materials Institute of Atomic and Molecular Science, Shaanxi University of Science and Technology, Xi'an 710021, China*
[c]*Department of Electronic Engineering, School of Electronic Information and Electrical Engineering, Shanghai Jiao Tong University, Shanghai 200240, China*

Received: January 15, 2022; Revised: May 22, 2022; Accepted: May 25, 2022

Abstract: The microstructure and morphology of Ti_3AlC_2 powders not only affect the preparation of Ti_3C_2 MXene but also have a great influence on their potential applications, such as microwave absorbers, alloy additives, or catalytic supports. However, the synthesis of Ti_3AlC_2 powders with desired microstructure and morphology remains a challenge. Herein, hollow Ti_3AlC_2 microrods were prepared for the first time in NaCl/KCl molten salts by using titanium, aluminum, and short carbon fibers as starting materials. It was found that the short carbon fibers not only performed as carbon source but also acted as sacrificial template. Furthermore, it was revealed that TiC and Ti_2AlC were initially formed on the surface of carbon fibers. The subsequent reactions between the outer Ti, Al and the inner carbon were dominated by the Kirkendall effect which gave rise to the formation of a hollow structure. Based on this mechanism, hollow Ti_3AlC_2 microspheres and a series of hollow TiC, Ti_2AlC, and V_2AlC powders were also successfully fabricated. This work provides a facile route to synthesize hollow MAX phases and may give enlightenment on preparing other hollow carbide powders via the Kirkendall effect in the molten salts.

Keywords: Ti_3AlC_2; molten salt synthesis (MSS); hollow structure; Kirkendall effect

1 Introduction

MAX phases represent a large family of inherently nanolaminate, hexagonal, and early transition-metal carbides or nitrides, which exhibit relatively high fracture toughness, easy machinability, oxidation resistance, and good electrical conductivity [1,2]. These particular properties make them attractive to many fields such as electrical contacts, catalysis, heat elements, protective coatings, and high-temperature structural applications [3–5]. Especially, with the discovery of MXenes in 2011 [6], the MAX phases have captured growing attention since they are the only precursors of MXenes [7,8]. Over the past ten years, the studies of MAX phases mainly focus on the development of new phases. For instance, a series of MAX phases, such as Ti_2ZnC,

* Corresponding author.
E-mail: liuyi@sust.edu.cn

Ti_3ZnC_2, Ti_2AuC, $Ti_3Au_2C_2$, Mo_2Ga_2C, V_2SnC, Sc_2SnC, Zr_2SeC, and Ti_2InB_2, were successfully synthesized [9–16]. In addition, lots of MAX phase solid solutions such as *o*-MAX, *i*-MAX, and even medium-/high-entropy MAX were also explored [17–22]. These works not only greatly enrich the members of the MAX phase family, but also provide diversified precursors for the preparation of MXenes.

In addition to serving as the precursors of MXenes, another potential application of MAX phase powders is microwave absorbers [23,24]. In this case, the morphology and microstructure of microwave absorbers are of great significance. For example, low-dimensional morphologies, hollow or hierarchical structures are proved to be beneficial to the improvement of microwave absorption performance [25–27]. However, it is difficult to fabricate the MAX phase powders with the above-mentioned microstructures since the conventional synthesis methods usually involve high-temperature solid reactions and pulverizations, which leads to the formation of irregular powders. Therefore, although plenty of MAX phases and their solid solutions have been explored, preparing the MAX phase powders with specific morphologies and hollow structures remains a big challenge.

Different from the conventional synthesis methods, molten salt synthesis (MSS) provides a liquid medium that can accelerate the reactions between the precursors and thus reduces the synthesis temperature [28–30]. Another advantage of MSS is that the powder materials can be obtained directly by water washing after reactions. This grinding-free method gives the possibility for the regulation of powder morphology. In recent years, several MAX phases including Cr_2AlC, V_2AlC, Ti_2AlC, Sc_2SnC, Ti_3SiC_2, Ti_3AlC_2, and $V_2(A_xSn_{1-x})C$ (A = Fe, Co, Ni, Mn) solid solutions have been synthesized successfully by the MSS at relative low temperatures [13,19,23,29,31–35]. In these works, the obtained MAX phase powders are irregular aggregates that consist of submicron-/nano-grains, and the morphology evolution during the MSS has been overlooked. However, it is demonstrated that, the formation of TiC in chloride molten salts is controlled by "carbon-template growth" mechanism, which means that the morphology of obtained TiC depends on the morphology of carbon precursors during the MSS [36,37]. Since TiC is an important interphase during the formation of Ti_2AlC or Ti_3AlC_2, it is anticipated that the morphologies of these phases may be regulated by using the carbon precursors with different shapes.

To verify this assumption, Ti_3AlC_2 powders were synthesized in the NaCl/KCl molten salts by using Ti, Al, and short carbon fibers as precursors. As expected, the rod-like Ti_3AlC_2 powders are obtained. However, the hollow structure is beyond our anticipation. Thus, the reaction process and morphology evolution are investigated, and the formation mechanism of the hollow structure is proposed.

2 Materials and method

Elemental powders of Ti (≥ 300 mesh, purity ≥ 99.99%, Aladdin Reagent Co., Ltd., China) and Al (200–400 mesh, purity ≥ 99.9%, Sinopharm Chemical Reagent Co., Ltd., China) were used as metal precursors. The short carbon fibers (Jilin Jiyan High-Tech Fibers Co., Ltd., China) were adopted as the carbon precursors. The NaCl and KCl mixtures (purity ≥ 99.5%, Aladdin Reagent Co., Ltd., China) were used as reaction media. Before using, NaCl and KCl were dried at 200 ℃ for 18 h to remove the residual moisture.

The starting materials were mixed with a molar ratio of Ti : Al : C : NaCl : KCl = 3 : 1.2 : 2 : 4 : 4, and the mixtures were ball-milled in ethanol for 10 h by using zirconia balls (Φ = 5 mm) as milling media. The obtained slurry was dried under a vacuum at 60 ℃ for 2 h and then transferred to alumina boats. Next, the boats were placed into a tube furnace and heated to 1250 ℃ with a heating rate of 4 ℃/min in a flowing Ar atmosphere. After holding for 9 h, the temperature was decreased to 600 ℃ at a rate of 2 ℃/min, and then naturally cooled to room temperature. The obtained samples were washed with deionized water to remove the residual NaCl/KCl salts and then dried at 80 ℃ for 12 h. To investigate the reaction mechanism during the MSS, the mixed powders were heated to 750–1250 ℃ without holding time and cooled to ambient temperature quickly.

The phase compositions were tested by an X-ray diffractometer (D8-Advance, Bruker, Germany) with Cu Kα radiation (λ = 0.15406 nm) in the range of 5°–70°. The purity of obtained Ti_3AlC_2 was estimated via Rietveld refinement. The morphologies and chemical compositions of obtained Ti_3AlC_2 powders and starting precursors were characterized via a field emission scanning electron microscope (Apreo S, FEI, USA) equipped with an energy dispersive X-ray spectrometer (EDS, NORAN System 7, Thermo Scientific, USA). To

obtain the internal structures, the obtained powders were embedded into the epoxy resin and cut into pieces, and then polished mechanically. On the other hand, to reveal the formation mechanism of the hollow structure, the unwashed products after reactions at different temperatures were also polished directly by Ar ions (697 Ilion Ⅱ, Gatan, USA) and examined by the SEM and EDS.

3 Results and discussion

Figure 1(a) shows the XRD pattern and Rietveld refinement of the sample synthesized at 1250 ℃ for 9 h. It can be seen that the obtained product is composed of Ti_3AlC_2 and a small amount of TiC. The relative content of Ti_3AlC_2 reaches up to 97.8%, indicating the high purity of the MSS method. Figure 1(b) shows that the obtained Ti_3AlC_2 powders exhibit a uniform rod-like morphology. However, when observing the internal structures from the cross-section images displayed in Figs. 1(c) and 1(d), it is surprising that the obtained Ti_3AlC_2 powders represent a hollow structure.

To reveal the formation of a rod-like and hollow structure, the microstructures of short carbon fibers are firstly observed and shown in Figs. S1(a) and S1(b) in the Electronic Supplementary Material (ESM). The statistical analysis of diameters for short carbon fibers and Ti_3AlC_2 microrods is also presented in Figs. S1(c)–S1(e) in the ESM. Obviously, the short carbon fibers have a uniform rod-like morphology, and their inside is solid, which indicates that the hollow structure of Ti_3AlC_2 microrods is formed during the synthesis process. Based on the statistical analysis of diameters shown in Figs. S1(c)–S1(e) in the ESM, the average sizes of short carbon fibers and Ti_3AlC_2 microrods along the radial direction are 7.05 and 13.17 μm, respectively. In addition, it should be noted that the internal diameter of Ti_3AlC_2 powders is 6.62 μm, which is very close to the diameter of short carbon fibers (7.05 μm). It means that the formation of Ti_3AlC_2 during the MSS may be initiated on the surface of short carbon fibers and extend radially outward. These results indicate that the short carbon fiber not only performed as carbon source but also acted as sacrificial template during the formation of Ti_3AlC_2.

To further clarify the formation mechanism of the hollow structure of Ti_3AlC_2 during the MSS, the starting mixtures were heated to 750–1250 ℃ without holding time, and the XRD patterns of the representative samples are shown in Fig. 2(a). It is apparent that,

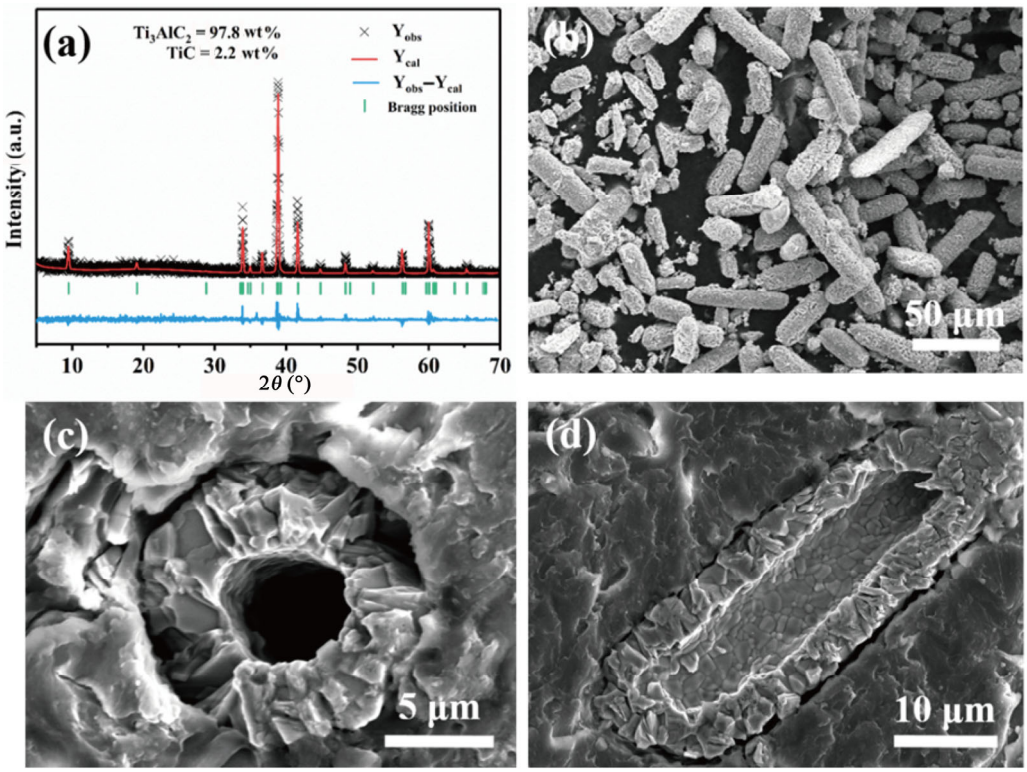

Fig. 1 XRD pattern and SEM images of obtained hollow Ti_3AlC_2 microrods: (a) XRD pattern, (b) overview of Ti_3AlC_2 microrods, and (c, d) cross-section of Ti_3AlC_2 microrods along the radial direction and along the length direction, respectively.

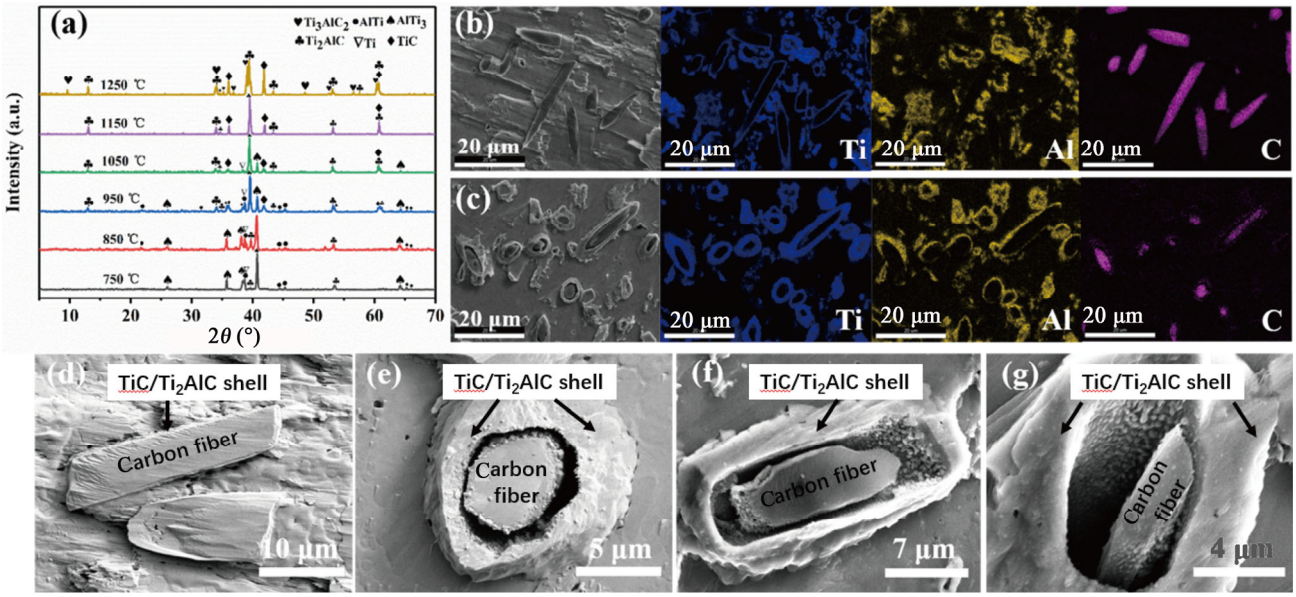

Fig. 2 (a) XRD patterns of samples synthesized at different temperatures without holding time; SEM images and elemental mappings of unwashed samples synthesized at (b) 950 ℃ and (c) 1150 ℃; and SEM images of unwashed samples synthesized at (d) 950 ℃, (e) 1050 ℃, (f) 1150 ℃ and (g) 1250 ℃.

when the reaction temperature is 750 ℃, the main phases in the product include Ti, Ti_3Al, TiAl, and a very small amount of Ti_2AlC. With the temperature increasing to 850 ℃, the content of Ti_2AlC in the product increases slightly. Meanwhile, a trace of TiC can be observed. When the temperature rises from 850 to 1050 ℃, the content of Ti_2AlC and TiC increases continuously, while the content of Ti, TiAl, and Ti_3Al decreases gradually. Until 1150 ℃, only Ti_2AlC and TiC are residual in the product. As the temperature reaches up to 1250 ℃, the Ti_3AlC_2 phase is present except for Ti_2AlC and TiC. From the above phase analysis, it is demonstrated that, the interphases, such as Ti_3Al, TiAl, TiC, and Ti_2AlC, show up before the formation of Ti_3AlC_2 during the MSS process of Ti_3AlC_2, which is consistent with the previous literature [33].

Figures 2(b)–2(g) show the SEM images and elemental mappings of unwashed samples which were synthesized at 950–1250 ℃ and directly polished by Ar ions. As can be seen from Fig. 2(b), the Ti and Al elements have a similar distribution in molten salt matrix. Especially, a thin layer of Ti and Al elements is observed along the surface of carbon fiber, indicating the formation of TiC/Ti_2AlC shell according to the analysis of XRD pattern. As the temperature increases to 1150 ℃, most of the Ti and Al elements are distributed along the surface of carbon fiber (Fig. 2(c)), which means that the reactions among Ti, Al, and C in the molten salts is a process wherein Ti and Al atoms diffuse to the surface of carbon fiber. Figures 2(d)–2(g) display the microstructural evolution as the temperature increases from 950 to 1250 ℃. It is obvious that the gap between the inner carbon fiber and the outer TiC/Ti_2AlC shell becomes larger as the reactions proceed, finally resulting in the formation of the hollow structure. It should be noted that plenty of small particles are present inside the gaps as shown in Figs. 2(e)–2(g). According to the element mappings (Fig. S2 in the ESM), these small particles are NaCl/KCl mixtures which may play an important role on the transportation of carbon atoms from the inner carbon fiber to the outer TiC/Ti_2AlC shell. These small particles may come from the molten salts that diffused into the surface of carbon fiber when the TiC/Ti_2AlC shell has not been completely formed at the initial stage of the reactions. This speculation can be confirmed by the element mappings of Na, K, and Cl in short carbon fibers after being treated in the NaCl/KCl molten salts (Fig. S3 in the ESM).

Based on the above analysis, the underlying formation mechanism of hollow Ti_3AlC_2 microrods is shown in Fig. 3. Firstly, when the temperature exceeds 700℃, NaCl, KCl, and Al have been melted. With the temperature increasing, the Ti particles begin to dissolve in the molten salts (Ti, Al, and NaCl/KCl molten salts are not shown in Fig. 3). Once the Ti and Al atoms diffuse to

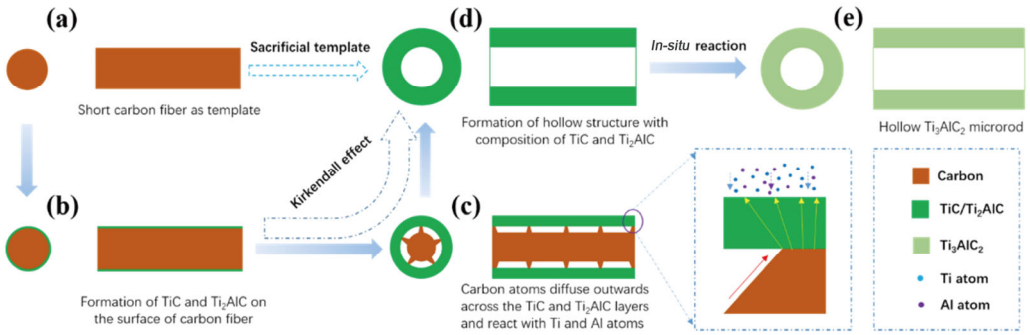

Fig. 3 Schematic diagram of formation mechanism of hollow Ti_3AlC_2 microrods.

the surface of carbon fiber, the reactions among Ti, Al, and C are occurred and give rise to the formation of TiC and Ti_2AlC on the surface of carbon fiber. As the reactions proceed, the carbon fiber is gradually covered by a shell of TiC/Ti_2AlC mixtures, which hinders the direct contact between the outer Ti, Al and the inner carbon fiber (Fig. 3(b)). In this situation, the reactions among Ti, Al, and C are determined by the atomic diffusion across the TiC/Ti_2AlC shell. From the Ti–C binary phase diagram, the composition of titanium carbide (TiC_y) can vary from $TiC_{0.48}$ to TiC [38], which means that a large number of C vacancies can exist in TiC lattice, and TiC could be recognized as a buffer pool for the diffusion of C atoms. On the other hand, the theoretical calculation shows that the Ti vacancies have the highest formation energy in Ti_2AlC lattice [39], indicating the sluggish diffusion of Ti atoms in Ti_2AlC. Therefore, once the TiC/Ti_2AlC shell is formed on the surface of carbon fiber, the subsequent reactions involve a process in which the C atoms continuously diffuse outward across the TiC/Ti_2AlC shell and react with the Ti and Al atoms on the outer surface (Fig. 3(c)). This is a typical Kirkendall effect that can lead to the formation of the hollow structure as reported in the previous literature [40]. When all Ti and Al in the molten salts react with C from the carbon fiber, the hollow TiC and Ti_2AlC shell is totally formed (Fig. 3(d)). As the temperature increases, the hollow TiC and Ti_2AlC shell transforms into the hollow Ti_3AlC_2 microrods through the *in-situ* reaction between TiC and Ti_2AlC (Fig. 3(e)). Based on this synthesis mechanism, the hollow Ti_3AlC_2 microspheres and a series of hollow TiC, Ti_2AlC, and V_2AlC powders are also synthesized (Fig. S4 in the ESM).

To evaluate the advantages of the hollow structure of Ti_3AlC_2, the microwave absorption properties were investigated. Figure 4 shows the reflection loss (RL) and effective absorption width (EAB) of Ti_3AlC_2 (45 wt%)/paraffin hybrids. It can be seen that the RL and EAB values can reach −53.48 dB (10.72 GHz, 2.30 mm) and 4.56 GHz (9.92–14.48 GHz, 2.1 mm), respectively. The above results are better than those in the reported literature in which the mass ratio of MAX phase powders is as high as 70% (Table S1 in the ESM). The reason for the enhancement of microwave absorption properties may be attributed to the hollow and rod-like structure, which is beneficial to the impedance matching and dielectric loss. A further in-depth investigation is needed in the future work.

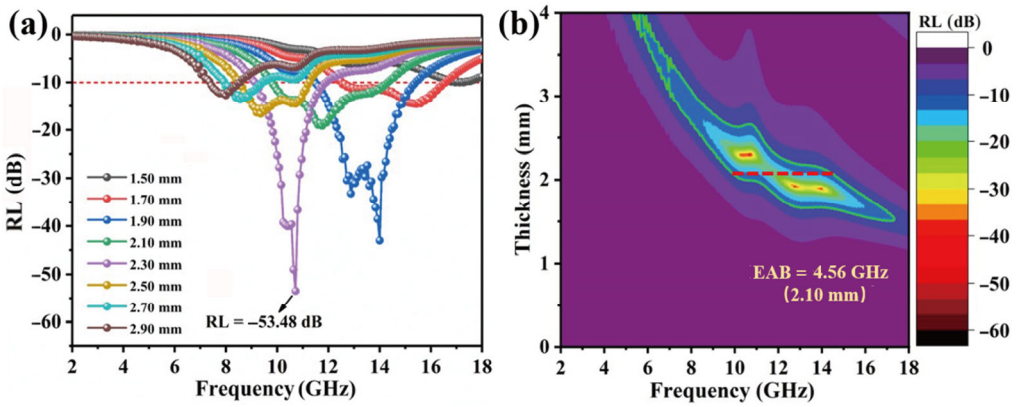

Fig. 4 Reflection loss and effective absorption width of Ti_3AlC_2 (45 wt%)/paraffin hybrids.

4 Conclusions

The hollow Ti_3AlC_2 microrods with high purity were successfully synthesized in the NaCl/KCl molten salts by using titanium, aluminum, and short carbon fibers as starting materials at 1250 ℃ for 9 h. It was found that the short carbon fibers not only performed as carbon source but also acted as sacrificial template. The formation mechanism of the hollow structure could be ascribed to the Kirkendall effect for which the interphases of TiC and Ti_2AlC played a role in the buffer pool for carbon diffusion. The obtained hollow Ti_3AlC_2 microrods exhibit good microwave absorption properties. Based on this mechanism, the hollow Ti_3AlC_2, Ti_2AlC, V_2AlC, and TiC powders were also successfully synthesized. This work is the first attempt to synthesize the micro-sized hollow MAX phases via the Kirkendall effect in the molten salts and may shed light on preparing other hollow carbides powders.

Acknowledgements

This work was supported by the National Natural Science Foundation of China (Grant Nos. 51602184 and 21902096), the Natural Science Foundation of Shaanxi Province (Grant No. 2020JM-505), and the Academic Talent Introduction Program of SUST (Grant No. 134080056).

Declaration of competing interest

The authors have no competing interests to declare that are relevant to the content of this article.

Electronic Supplementary Material

Supplementary material is available in the online version of this article at https://doi.org/10.1007/s40145-022-0616-0.

References

[1] Gonzalez-Julian J. Processing of MAX phases: From synthesis to applications. *J Am Ceram Soc* 2021, **104**: 659–690.

[2] Zhang H, Hu T, Wang XH, *et al*. Structural defects in MAX phases and their derivative MXenes: A look forward. *J Mater Sci Technol* 2020, **38**: 205–220.

[3] Fu L, Xia W. MAX phases as nanolaminate materials: Chemical composition, microstructure, synthesis, properties, and applications. *Adv Eng Mater* 2021, **23**: 2001191.

[4] Eklund P, Rosen J, Persson POÅ. Layered ternary $M_{n+1}AX_n$ phases and their 2D derivative MXene: An overview from a thin-film perspective. *J Phys D*: *Appl Phys* 2017, **50**: 113001.

[5] Zhou AG, Liu Y, Li SB, *et al*. From structural ceramics to 2D materials with multi-applications: A review on the development from MAX phases to MXenes. *J Adv Ceram* 2021, **10**: 1194–1242.

[6] Naguib M, Kurtoglu M, Presser V, *et al*. Two-dimensional nanocrystals produced by exfoliation of Ti_3AlC_2. *Adv Mater* 2011, **23**: 4248–4253.

[7] Sokol M, Natu V, Kota S, *et al*. On the chemical diversity of the MAX phases. *Trends Chem* 2019, **1**: 210–223.

[8] Li M, Huang Q. Recent progress and prospects of ternary layered carbides/nitrides MAX phases and their derived two-dimensional nanolaminates MXenes. *J Inorg Mater* 2020, **35**: 1–7. (in Chinese)

[9] Xu Q, Zhou YC, Zhang HM, *et al*. Theoretical prediction, synthesis, and crystal structure determination of new MAX phase compound V_2SnC. *J Adv Ceram* 2020, **9**: 481–492.

[10] Lu YF, Khazaei M, Hu XM, *et al*. Facile synthesis of Ti_2AC (A = Zn, Al, In, and Ga) MAX phases by hydrogen incorporation into crystallographic voids. *J Phys Chem Lett* 2021, **12**: 11245–11251.

[11] Hu C, Lai CC, Tao Q, *et al*. Mo_2Ga_2C: A new ternary nanolaminated carbide. *Chem Commun* 2015, **51**: 6560–6563.

[12] Li M, Li YB, Luo K, *et al*. Synthesis of novel MAX phase Ti_3ZnC_2 via A-site-element-substitution approach. *J Inorg Mater* 2019, **34**: 60–64. (in Chinese)

[13] Li YB, Qin YQ, Chen K, *et al*. Molten salt synthesis of nanolaminated Sc_2SnC MAX phase. *J Inorg Mater* 2021, **36**: 773–778. (in Chinese)

[14] Fashandi H, Dahlqvist M, Lu J, *et al*. Synthesis of Ti_3AuC_2, $Ti_3Au_2C_2$ and Ti_3IrC_2 by noble metal substitution reaction in Ti_3SiC_2 for high-temperature-stable Ohmic contacts to SiC. *Nat Mater* 2017, **16**: 814–818.

[15] Wang JJ, Ye TN, Gong YT, *et al*. Discovery of hexagonal ternary phase Ti_2InB_2 and its evolution to layered boride TiB. *Nat Commun* 2019, **10**: 2284.

[16] Chen K, Bai XJ, Mu XL, *et al*. MAX phase Zr_2SeC and its thermal conduction behavior. *J Eur Ceram Soc* 2021, **41**: 4447–4451.

[17] Liu ZM, Wu ED, Wang JM, *et al*. Crystal structure and formation mechanism of $(Cr_{2/3}Ti_{1/3})_3AlC_2$ MAX phase. *Acta Mater* 2014, **73**: 186–193.

[18] Tao QZ, Dahlqvist M, Lu J, *et al*. Two-dimensional $Mo_{1.33}C$ MXene with divacancy ordering prepared from parent 3D laminate with in-plane chemical ordering. *Nat Commun* 2017, **8**: 14949.

[19] Li YB, Lu J, Li M, *et al*. Multielemental single-atom-thick *A* layers in nanolaminated $V_2(Sn, A)C$ (*A* = Fe, Co, Ni, Mn) for tailoring magnetic properties. *P Natl Acad Sci USA* 2020, **117**: 820–825.

[20] Bao WC, Wang XG, Ding HJ, *et al*. High-entropy M_2AlC–MC (M = Ti, Zr, Hf, Nb, Ta) composite: Synthesis and

microstructures. *Scripta Mater* 2020, **183**: 33–38.

[21] Liu C, Yang YY, Zhou ZF, *et al*. $(Ti_{0.2}V_{0.2}Cr_{0.2}Nb_{0.2}Ta_{0.2})_2AlC$–$(Ti_{0.2}V_{0.2}Cr_{0.2}Nb_{0.2}Ta_{0.2})C$ high-entropy ceramics with low thermal conductivity. *J Am Ceram Soc* 2022, **105**: 2764–2771.

[22] Chen K, Chen YH, Zhang JN, *et al*. Medium-entropy (Ti, Zr, Hf)$_2$SC MAX phase. *Ceram Int* 2021, **47**: 7582–7587.

[23] Luo W, Liu Y, Wang CY, *et al*. Molten salt assisted synthesis and electromagnetic wave absorption properties of $(V_{1-x-y}Ti_xCr_y)_2AlC$ solid solutions. *J Mater Chem C* 2021, **9**: 7697–7705.

[24] Shi YM, Luo F, Liu Y, *et al*. Preparation and microwave absorption properties of Ti_3AlC_2 synthesized by pressureless sintering TiC/Ti/Al. *Int J Appl Ceram Technol* 2014, **12**: E172–E177.

[25] Yuan XY, Wang RQ, Huang WR, *et al*. Lamellar vanadium nitride nanowires encapsulated in graphene for electromagnetic wave absorption. *Chem Eng J* 2019, **378**: 122203.

[26] Xie S, Ji ZJ, Zhu LC, *et al*. Recent progress in electromagnetic wave absorption building materials. *J Build Eng* 2020, **27**: 100963.

[27] Li M, Han MK, Zhou J, *et al*. Novel scale-like structures of graphite/TiC/Ti_3C_2 hybrids for electromagnetic absorption. *Adv Elec tron Mater* 2018, **4**: 1700617.

[28] Liu XF, Fechler N, Antonietti M. Salt melt synthesis of ceramics, semiconductors and carbon nanostructures. *Chem Soc Rev* 2013, **42**: 8237–8265.

[29] Dash A, Vaßen R, Guillon O, *et al*. Molten salt shielded synthesis of oxidation prone materials in air. *Nat Mater* 2019, **18**: 465–470.

[30] Gupta SK, Mao YB. A review on molten salt synthesis of metal oxide nanomaterials: Status, opportunity, and challenge. *Prog Mater Sci* 2021, **117**: 100734.

[31] Dash A, Sohn YJ, Vaßen R, *et al*. Synthesis of Ti_3SiC_2 MAX phase powder by a molten salt shielded synthesis (MS^3) method in air. *J Eur Ceram Soc* 2019, **39**: 3651–3659.

[32] Wang BX, Zhou AG, Hu QK, *et al*. Synthesis and oxidation resistance of V_2AlC powders by molten salt method. *Int J Appl Ceram Technol* 2017, **14**: 873–879.

[33] Liu HJ, Wang Y, Yang LX, *et al*. Synthesis and characterization of nanosized Ti_3AlC_2 ceramic powder by elemental powders of Ti, Al and C in molten salt. *J Mater Sci Technol* 2020, **37**: 77–84.

[34] Galvin T, Hyatt NC, Rainforth WM, *et al*. Molten salt synthesis of MAX phases in the Ti–Al–C system. *J Eur Ceram Soc* 2018, **38**: 4585–4589.

[35] Roy C, Banerjee P, Bhattacharyya S. Molten salt shielded synthesis (MS^3) of Ti_2AlN and V_2AlC MAX phase powders in open air. *J Eur Ceram Soc* 2020, **40**: 923–929.

[36] Yan MG, Xiong QM, Huang JT, *et al*. Molten salt synthesis of titanium carbide using different carbon sources as templates. *Ceram Int* 2021, **47**: 17589–17596.

[37] Nadimi H, Soltanieh M, Sarpoolaky H. The formation mechanism of nanocrystalline TiC from KCl–LiCl molten salt medium. *Ceram Int* 2020, **46**: 18725–18733.

[38] Gusev AI. Phase equilibria, phases and chemical compounds in the Ti–C system. *ChemInform* 2002, **33**: 222.

[39] Liao T, Wang JY, Zhou YC. *Ab initio* modeling of the formation and migration of monovacancies in Ti_2AlC. *Scripta Mater* 2008, **59**: 854–857.

[40] Yin YD, Rioux RM, Erdonmez CK, *et al*. Formation of hollow nanocrystals through the nanoscale Kirkendall effect. *Science* 2004, **304**: 711–714.